New Journal of Physics
The open access journal at the forefront of physics

Deutsche Physikalische Gesellschaft DPG IOP Institute of Physics

PAPER • OPEN ACCESS

High order plasmonic vortex generation based on spiral nanoslits

To cite this article: Jing Fang *et al* 2021 *New J. Phys.* **23** 033013

View the article online for updates and enhancements.

You may also like

- Single nano-hole as a new effective nonlinear element for third-harmonic generation
P N Melentiev, T V Konstantinova, A E Afanasiev et al.
- Control of SPP propagation and focusing through scattering from nanostructures
P.N. Melentiev, A.A. Kuzin and V.I. Balykin
- spiral nanoslit and the higher order plasmonic vortex generation
Xiaoqing Lu, Yuansheng Han, Haoran Lv et al.

This content was downloaded from IP address 152.15.112.8 on 10/07/2023 at 20:46

New Journal of Physics
The open access journal at the forefront of physics

Deutsche Physikalische Gesellschaft DPG
IOP Institute of Physics

Published in partnership with: Deutsche Physikalische Gesellschaft and the Institute of Physics

OPEN ACCESS

RECEIVED
1 December 2020

REVISED
6 February 2021

ACCEPTED FOR PUBLICATION
17 February 2021

PUBLISHED
10 March 2021

Original content from this work may be used under the terms of the Creative Commons Attribution 4.0 licence.

Any further distribution of this work must maintain attribution to the author(s) and the title of the work, journal citation and DOI.

PAPER

High order plasmonic vortex generation based on spiral nanoslits

Jing Fang[1], Changda Zhou[1], Zhen Mou[1], Shuyun Wang[1], Jiayi Yu[1], Yuanjie Yang[2], Gregory J Gbur[3], Shuyun Teng[1,*] and Yangjian Cai[1,*]

[1] Shandong Provincial Key Laboratory of Optics and Photonic Device & School of Physics and Electronics, Shandong Normal University, Jinan 250014, People's Republic of China
[2] School of Astronautics and Aeronautics, University of Electronic Science and Technology of China, Chengdu 611731, People's Republic of China
[3] Department of Physics and Optical Science, University of North Carolina at Charlotte, Charlotte, North Carolina 28223, United States of America
[*] Authors to whom any correspondence should be addressed.

E-mail: tengshuyun@sdnu.edu.cn and yangjiancai@sdnu.edu.cn

Keywords: plasmonic vortex, nanostructure, topological charge, near-field diffraction

Abstract

Highly localized plasmonic vortices carrying orbital angular momentum are of importance for many applications. Yet, it is a challenge to generating plasmonic vortex with a high topological charge because of no available technique. Here, a novel plasmonic vortex generator is proposed based on spiral nanoslits etched in a metal film, which can produce a high order plasmonic vortex. The consecutive spiral nanoslit can generate plasmonic vortex with high intensity and the segmented nanoslits enhances the controllability of the plasmonic vortex, which are demonstrated numerically and experimentally. High order plasmonic vortex generation will broaden the prospects for plasmonic vortices in practical applications for nanomanipulation and nanofabrication.

1. Introduction

Optical vortex is used to describe a light field possessing a helical wave front and a doughnut-shaped intensity distribution in its cross-section. Since vortex beam possesses orbital angular momentum (OAM) and vortex beams with different topological charges may be multiplexed and demultiplexed, studies of vortex beams have attracted much attention in the fields of optical communication [1, 2], particle trapping [3, 4], nanofabrication [5] and quantum information processing [6, 7]. Generally, the phase of an optical vortex can be expressed by a term of $\exp(jm\varphi)$, where φ is the azimuthal angle and m denotes the topological charge corresponding to the order of the optical vortex [8]. Optical vortices with different orders have been produced by using various methods including cylindrical lenses [9], spiral phase plate [10], spatial light modulator [11] and optical wave-guide [12].

Recently, plasmonic vortices (PVs) have aroused a lot of interest due to their high localization. Different from the far-field optical vortices, PVs result from the superposition of surface plasmon polaritons (SPPs) or the surface waves excited by nanostructures. Most of the above-mentioned methods are unavailable for generating the PVs. Thus, various nanostructures have been proposed to generate PVs and they are spiral nanoslits [13–16], single and double ring distributed nanoslits [17–19] and metasurface geometries [20–22]. Among these methods, a spiral slit has the advantage of being a simple structure that is convenient to manufacture and the generated PVs have high intensity. Nevertheless, high order PVs generated by a common spiral such as Archimedes spiral or Fermat's spiral have poor quality because of the damp effect of SPPs. Even for the Archimedes spirals with multiple arms [13, 23], the generated PVs are not ideal because of the interference effect of the deuterogenic field [24]. In our former work, we propose α spiral and the topological charge of the PV modified passively by α spiral still takes the limited value [25, 26]. This is the reason that spiral slits are rarely used in the generation of the higher order PVs.

© 2021 The Author(s). Published by IOP Publishing Ltd on behalf of the Institute of Physics and Deutsche Physikalische Gesellschaft

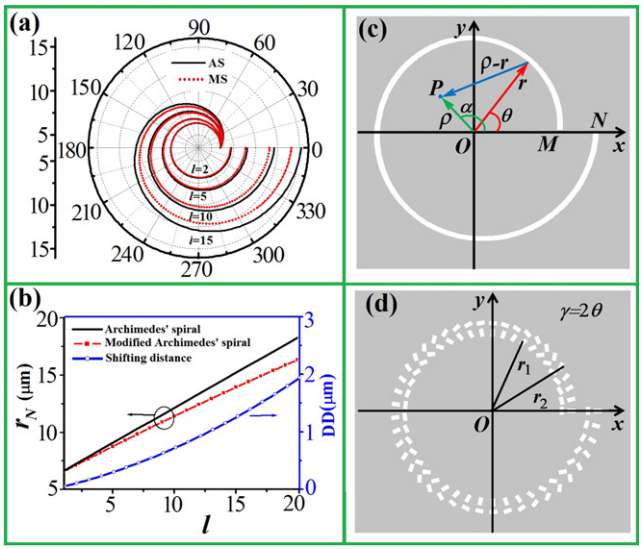

Figure 1. (a) Trajectories of Archimedes spirals (AS) and the modified spirals (MS) with l taking 2, 5, 10 and 15, (b) the end positions of two spirals (r_N) and their distance difference (DD), and (c) the proposed consecutive and (d) segmented spiral nanostructures.

The aim of this work is to explore simple spiral nanostructures to generate high order PVs carrying large OAM. The SPP fields excited by the proposed spirals actively compensate the damp effect of SPPs during the propagation. The spiral nanostructure may be consecutive or segmented nanoslits. The consecutive spiral nanoslit can generate high order PV with high intensity and the segmented nanoslit structure further increases the topological charge of the generated PV without increasing the size of nanostructure. The design principle provides the spiral trajectory of the proposed spiral nanostructures. The effective compensation of the damped SPPs by using the compressed spirals makes the generated high order PVs have high quality. The numerical simulations and experimental measurement verify the performance of the proposed spiral structures. This works paves a road for the generation of higher order PVs by a simple spiral and it will bring more possibility for expanding the applications of PVs in optical micro-manipulation, integrated optical coding and nanofabrication.

2. Design principle

An ideal optical vortex with the topological charge of m has annular intensity distribution and its phase uniformly changes m times of 2π around the phase singularity. In order to generate one ideal PV carrying larger OAM, the amplitude and phase of SPPs contributing to the formation of PV are the key factors. As we know, the phase of SPPs may be introduced through the propagation distance or by using the rotation of nanounits, and the amplitude damp of SPPs during the longer distance propagation cannot be neglected. Combining the exponential damp rule of SPPs along the interface of the metal and vacuum, we propose a modified spiral structure on basis of the common Archimedes spiral, and the trajectory of this spiral can be expressed by

$$r = r_0 + \frac{l\lambda_{\mathrm{spp}}\theta}{2\pi}\left[2 - \exp\left(\frac{l\lambda_{\mathrm{spp}}}{2\pi a}\right)\right], \tag{1}$$

where r_0 is the initial radius and the integer l denotes the geometrical charge of the spiral slit, λ_{spp} is the SPP wavelength. The parameter a depends on the metal material. Here, the radius r of spiral linearly increases with the angular coordination of θ. If we temporarily neglect the damp effect of SPPs, the parameter of a takes the infinite and the above expression can be simplified into the denotation of an Archimedes spiral, namely, $r = r_0 + l\theta\lambda_{\mathrm{spp}}/2\pi$. The difference between the modified spiral and Archimedes spiral can be seen from the curves shown in figures 1(a) and (b), where the value of l takes 2, 5, 10 and 15. The black solid and red dash lines denote the Archimedes spirals and the modified spirals, respectively.

It can be seen that the trajectories of the modified spiral and Archimedes spiral overlap as the geometrical charge of l takes 2. Their difference gets obvious with increase of l. The modified spiral seems to be radially compressed with respect to the Archimedes spiral, and the gap of the modified spiral between the start and the end is smaller than that of the Archimedes spiral with the same geometric charge. The variation of the spiral end with the value of l can be clearly seen from the curves given in figure 1(b), where

the distance difference of the end positions for Archimedes spiral and the modified spiral are also given. Obviously, the modification of the spiral with larger geometric charge is much larger.

The SPPs excited by the spiral consecutive nanoslit with the circularly polarized light illumination propagate towards the center of spiral nanoslit, like the case shown in figure 1(c), and their superposition at the position near the center can be calculated approximately through the integration operation

$$E(\rho,\alpha,z)=\int A_0\,\mathrm{e}^{-\kappa z-R/\delta_{\mathrm{spp}}}\,\mathrm{e}^{\mathrm{j}[\pm\theta+k_{\mathrm{spp}}r-k_{\mathrm{spp}}\rho\,\cos(\alpha-\theta)]}\,\mathrm{d}\theta. \tag{2}$$

Here, r and θ denote the radial and azimuthal coordinates of a small section of nanoslit, ρ, α and z are the radial, azimuthal and vertical coordinates of the observation point P near the center. A_0 equals to $E_0/(jR\lambda_{\mathrm{spp}})$ with E_0 denoting the amplitude of the incident field and $R=|\boldsymbol{\rho}-\boldsymbol{r}|=[\rho^2+r^2-2\rho r\cos(\alpha-\theta)]^{1/2}$ representing the distance from the slit to the observation point. k_{spp} is the wave number of SPPs, κ is the damped factor, and they satisfy $k_{\mathrm{spp}}=(k_0{}^2-\kappa^2)^{1/2}$ with k_0 the wave number in vacuum. δ_{spp} is the attenuation distance of the SPPs along the smoothing metal surface, which satisfies the relation of $\delta_{\mathrm{spp}}=\varepsilon_{\mathrm{r}}{}^2[(\varepsilon_{\mathrm{r}}+1)/\varepsilon_{\mathrm{r}}]/(k_0\varepsilon_{\mathrm{i}})$, where ε_{r} and ε_{i} denote the real and imaginary part of the dielectric function of silver.

The plus sign in the second exponential term of equation (2) is for the left-handed circular polarization (LCP) and the minus sign is for the right-handed circular polarization (RCP). Suppose the amplitudes of all SPP fields are the same, the above integration can be deduced into the following form

$$E(\rho,\alpha,z)\propto \mathrm{e}^{\mathrm{j}(l\pm1)\alpha}J_{l\pm1}(k_{\mathrm{spp}}\rho), \tag{3}$$

where J_i represents the ith order Bessel function. The spiral phase indicates that the optical field is a vortex of $l\pm1$ order. Theoretically, the PV of any order can be generated by the spiral nanoslit even when l takes larger values. Actually, the damp of SPPs gets obvious as l is larger and the generated vortex has poor quality. This is the reason for proposing the modified spiral to generate the high order PV. The modification of the spiral trajectory effectively offset the damp effect of SPP field.

For the consecutive spiral nanoslit with larger geometrical charge, the size of spiral is larger because of the larger gap. If a consecutive spiral slit is replaced by multiple nanoslit segments locating on the modified spiral trajectory, these short nanoslits can rotate around their center to introduce the additional phase though the intensity of optical field may decrease. When the nanoslit with the coordinates of r and θ rotates an angle of γ, the SPP field excited by this nanoslit is proportional to $\exp(j\sigma\gamma)\cos(\theta-\gamma)$, where $\sigma=\pm1$ with the positive sign for the LCP and the negative sign for the RCP. When the segmented nanoslits are arranged on two parallel trajectories with the separation of $\lambda_{\mathrm{SPP}}/2$ and two adjacent nanoslits are orthogonal, as shown in figure 1(d), the SPP field excited by two nanoslits with the same angular coordinate of θ is proportion to $\exp[j\sigma(2\gamma-\theta)]$ [26]. Thus, insert this expression into equation (2) and let γ equal to $n\theta$, the generated SPP field by all the nanoslits can be deduced into

$$E(\rho,\alpha,z)\propto \mathrm{e}^{\mathrm{j}[l\pm(2n-1)]\alpha}J_{l\pm(2n-1)}(k_{\mathrm{spp}}\rho). \tag{4}$$

Obviously, the PV with the topological charge taking $l\pm(2n-1)$ is formed. We rewrite this topological charge into the $l\pm1\pm2(n-1)$. This result indicates that the topological charge of the generated PV includes three parts. The first part of l comes from the geometrical charge of the spiral trajectory, the number 1 reflects the contribution of the incident circular polarization carrying the spin angular momentum and the third part of $2(n-1)$ corresponds to the contribution of the rotated nanoslits. Therefore, the segmented nanoslits can further increase the topological charge of the generated PV through the rotation of nanoslits without increasing the size of spiral nanostructure.

3. Numerical simulations

In order to verify the availability of our proposed spiral nanostructures for the generation of high order PVs, we simulate numerically the near-field diffraction of the proposed spiral nanostructures. For comparison, the diffraction by Archimedes spiral nanoslit is also simulated and figure 2(a) gives the diffraction intensity and phase distributions of Archimedes spiral nanoslit with $l=5$, where the nanoslit is etched in the silver film with the thickness taking 150 nm. The initial radius of spiral is 6 μm and the slit width is 200 nm. The illuminating light is the LCP light with the wavelength of 633 nm.

One can see that the simulated results show the intensity distribution is not uniform and the phase pattern is not symmetric. The central bright ring among the intensity pattern seems to have an opening on the top and one first-order phase singularity away from the center interferes the phase change along the azimuthal direction, as shown by the inserted arrows. These cases indicate the formed optical field deviates

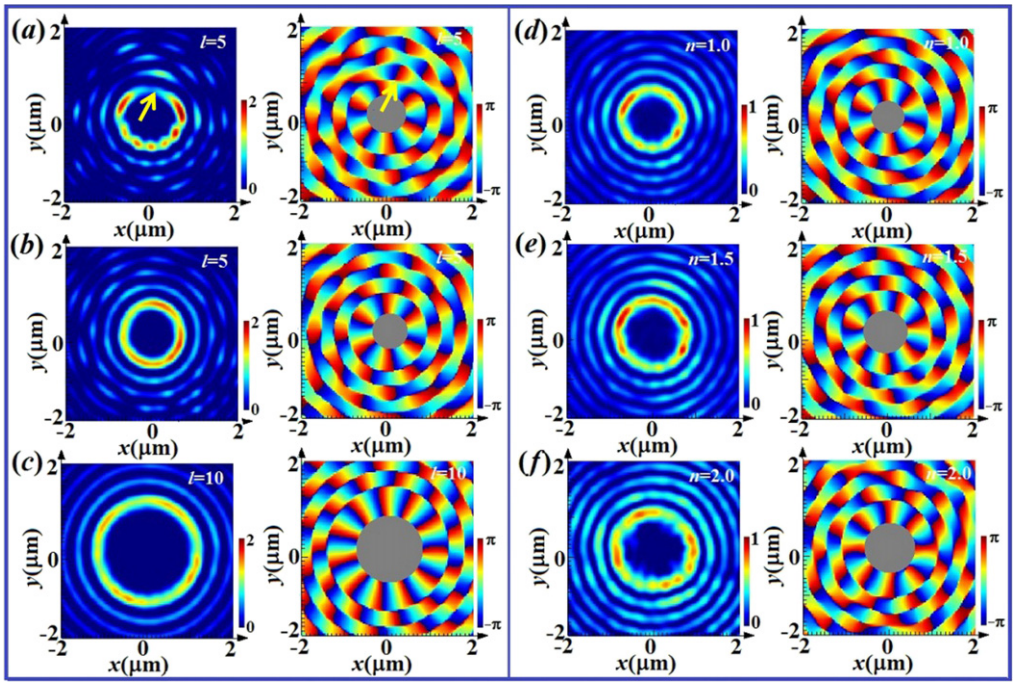

Figure 2. Diffraction intensity and phase distributions of (a) Archimedes spiral slits with $l = 5$, [(b) and (c)] the proposed spiral slits with $l = 5$ and 10, and the segmented nanoslits with the rotation parameters satisfying (d) $n = 1.0$, (e) 1.5 and (f) 2.0, where the illumination light takes the LCP.

from the pure integral vortex. More simulations show that the deviation gets severer with increase of the geometrical charge. This kind of field may cause abnormal behavior in practical applications, such as an abrupt acceleration of trapped nanometer particles.

Based on our proposed spiral model, we simulate the intensity and phase distributions of the modified spiral nanoslits and figures 2(b) and (c) give the results with $a = 28$ μm and $l = 5$ and 10 under the LCP light illumination. From figure 2(b), one can see that the intensity distribution is the annular shape and the phase uniformly changes 6 times of 2π in anticlockwise direction. These results indicate that the generated optical vortices are the ideal 6-order PVs, which is better than the one generated by Archimedes spiral. Figure 2(c) show the intensity distribution is the annular shape and the phase uniformly changes 11 times of 2π. These results verify the active modification of spiral trajectory is valid for the generation of high order PV. In fact, the ideal PV with the topological charge no less than 20 can be obtained because of the compensation of the damped SPP field.

Figures 2(d)–(f) give the simulated intensity and phase distributions of segmented nanoslits with the rotation angle taking $\gamma = \theta$, 1.5θ and 2θ and the parameters of spiral trajectory taking the same values as figure 2(b). From the intensity distributions, it is easy to see that the central bright ring gets larger with increase of the ratio of γ to θ. The phase distributions confirm that topological charge changes from 6, 7 to 8. The topological charge of the generated vortex satisfies the relation of $l + 1 + 2(n - 1)$. With comparison to figure 2(b), the segmented spiral structure increases the topological charge of the generated PV. This is consistent with the theoretical prediction. It needs to be pointed out that for ensuring the equivalent intensity of SPP field excited by the segmented nanoslit with different radial coordinate, the length of the segmented nanoslit increases from 300 nm to 550 nm with increase of its angular coordinate.

All these results are obtained by using the finite difference time domain method [27–29]. The spiral nanostructures are etched in the silver film with the thickness taking 150 nm and the SPP wavelength equals to $\lambda_{spp} = 613$ nm for the illuminating wavelength of 633 nm. The complex dielectric constant of silver is taken from the value given by Palik [30]. The perfectly matched layer is chosen as the adsorbing boundary and the minimum mesh cell takes 2 nm. The calculation region is set 20 μm $\times$ 20 μm $\times$ 6 μm and the monitor plane is set at 200 nm above the silver film. The incident polarization takes the LCP. For the RCP, the generated vortex by any spiral nanostructure is similar to the one with LCP light illumination except that the topological charge is smaller 2 than the latter.

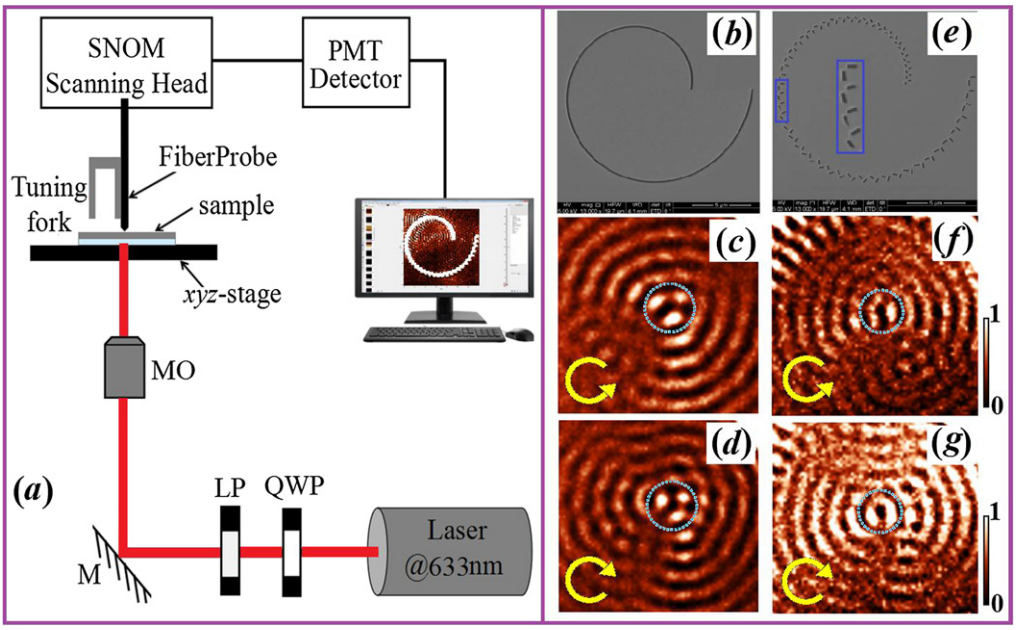

Figure 3. (a) Experiment setup, [(b) and (e)] SEM pictures of the fabricated Archimedes spiral slit of $l = 10$ with the width and the initial radius taking 200 nm and 6 μm, and the proposed spiral nanoslits with the length taking the value from 300 nm to 550 nm, and the intensity distributions with [(c) and (d)] the LCP and [(f) and (g)] RCP light illumination. Where the inserted nanostructure in (e) is the enlarged part of the segmented nanoslits and the inserted arrows in [(c), (d), (f) and (g)] denote the incident polarization.

4. Experiment measurement

The practical experiment is performed to testify the high order PV generation based on the proposed spiral nanostructure. The experiment includes the preparation of the samples and the measurement of the near-field diffraction. The preparation process of the sample contains the film deposition and the nanoslit fabrication. The metal film deposited onto the glass substrate is achieved with the help of the magnetron sputtering method. The metasurface sample is fabricated by the focused ion beam etching method. For comparison, we manufacture two samples. The first sample is an Archimedes spiral slit with the width and the initial radius taking 200 nm and 6 μm, and the second one is a proposed spiral nanostructure consisting of segmented nanoslits with the width taking 200 nm and the length taking the unequal values from 300 nm to 550 nm. The rotation angle of nanoslit and its position angle satisfy the relation of $\gamma = 1.5\theta$. The geometric charge of two spirals takes $l = 10$. Figures 3(b) and (e) give the scanning electron microscopy (SEM) images of two samples.

Put one fabricated sample into the light path of figure 3(a), we detect its diffraction intensity distribution by using the scanning near-field optical microscopy. The linearly polarized light with the wavelength of 633 nm emitted from the laser passes through the combination of a linear polarizer and a quarter wave plate, and then turns into the LCP or RCP light. A 20 $\times$ microscope objective is used to focus the incident light on the sample. The fiber probe collects the light field behind the nanostructure and transmit it to the detector. Finally, the near-field diffraction intensity pattern is output on the screen or recorded in the file. Figures 3(c) and (d) are the measured intensity distributions of the Archimedes spiral nanoslit with LCP and RCP light illumination, and figures 3(f) and (g) are the measured intensity distributions of the segmented nanoslits located on the modified spiral trajectory. Where the arrows inserted in patterns denote the incident polarization, and for convenience, the regions circled by the dashed lines highlight the difference of the optical fields near the center.

From figures 3(c) and (d), we can see that the intensity distributions near the center consist of three discrete spots, and these distributions deviate seriously the ideal PVs, like the theoretical prediction. Differently, the intensity distributions near the center of figures 3(f) and (g) close to the annular shape. Though the annular shapes are not perfect due to the manufacturing precision, they still indicate the quality of the generated PVs has been improved by using the segmented nanoslits at the modified spiral trajectory. Because of the opposite contributions coming from the spin orbit momentum carried by the incident circular polarization, the sizes of the discrete spots in figure 3(c) and the annular distribution in figure 3(f) are larger than those in figures 3(d) and (g). That means the topological charge of PV for the LCP light illumination is larger than the case for the RCP light illumination.

5. Conclusions

In summary, we explore theoretically and experimentally the generation of high order PVs based on spiral nanoslits. The proposed empirical expression for the spiral provides the theoretical basis for actively generating high order PVs with high quality under circularly polarized light illumination. Two kinds of spiral nanostructures including the consecutive and segmented nanoslits provide more choices to generate the PV carrying larger OAM. Numerical simulations and experiment measurement verify the availability of our proposed spiral nanostructures for the high order PV generation. The study of this article breaks the limitation of the spiral slit in generating the PV with larger topological charge, and the proposed spiral nanostructures pave a path to generate the high order PVs by using the simple spiral structure. We believe this work must be helpful for promoting the applications of PVs carrying larger OAM in more relevant fields.

Acknowledgments

Authors thanks the support by National Natural Science Foundation of China (10874105, 62002208) and Shandong Provincial Natural Science Foundation (ZR2020KA009).

Data availability statement

All data that support the findings of this study are included within the article (and any supplementary files).

Disclosures

The authors declare no conflicts of interest.

ORCID iDs

Jing Fang https://orcid.org/0000-0002-3854-5909
Zhen Mou https://orcid.org/0000-0001-9263-5481
Shuyun Wang https://orcid.org/0000-0002-9026-9489
Shuyun Teng https://orcid.org/0000-0001-6071-963X

References

[1] Jia P, Yang Y, Min C J, Fang H and Yuan X-C 2013 Sidelobe-modulated optical vortices for free-space communication *Opt. Lett.* **38** 588–90
[2] Willner A E *et al* 2015 Optical communications using orbital angular momentum beams *Adv. Opt. Photon.* **7** 66–106
[3] Williams S J, Kumar A, Green N G and Wereley S T 2009 A simple, optically induced electrokinetic method to concentrate and pattern nanoparticles *Nanoscale* **1** 133–7
[4] Ng J, Lin Z F and Chan C T 2010 Theory of optical trapping by an optical vortex beam *Phys. Rev. Lett.* **104** 103601
[5] Toyoda K, Miyamoto K, Aoki N, Morita R and Omatsu T 2012 Using optical vortex to control the chirality of twisted metal nanostructures *Nano Lett.* **12** 3645–9
[6] Nicolas A, Veissier L, Giner L, Giacobino E, Maxein D and Laurat J 2014 A quantum memory for orbital angular momentum photonic qubits *Nat. Photon.* **8** 234–8
[7] Ding D S, Zhang W, Zhou Z Y, Shi S, Xiang G Y, Wang Z S, Jiang Y K, Shi B S and Guyo G C 2014 Quantum storage of orbital angular momentum entanglement in an atomic ensemble *Phys. Rev. Lett.* **114** 050502
[8] Yao A M and Padgett M J 2011 Orbital angular momentum: origins, behavior and applications *Adv. Opt. Photon.* **3** 161–204
[9] Beijersbergen M W, Allen L, Van der Veen H and Woerdman J P 1993 Astigmatic laser mode converters and transfer of orbital angular momentum *Opt. Commun.* **96** 123–32
[10] Kotlyar V V, Elfstrom H, Turunen J, Almazov A A, Khonina S N and Soifer V A 2005 Generation of phase singularity through diffracting a plane or Gaussian beam by a spiral phase plate *J. Opt. Soc. Am.* A **22** 849–61
[11] Ostrovsky A S, Rickenstorff-Parrao C and Arrizón V 2013 Generation of the 'perfect' optical vortex using a liquid-crystal spatial light modulator *Opt. Lett.* **38** 534–6
[12] Cai X, Wang J, Strain M J, Johnson-Morris B, Zhu J, Sorel M, O'Brien J L, Thompson M G and Yu S 2012 Integrated compact optical vortex beam emitters *Science* **338** 363–6
[13] Kim H, Park J, Cho S-W, Lee S-Y, Kang M and Lee B 2010 Synthesis and dynamic switching of surface plasmon vortices with plasmonic vortex lens *Nano Lett.* **10** 529–36
[14] Cho S-W, Park J, Lee S-Y, Kim H and Lee B 2012 Coupling of spin and angular momentum of light in plasmonic vortex *Opt. Express* **20** 10083–94
[15] Spektor G *et al* 2017 Revealing the subfemtosecond dynamics of orbital angular momentum in nanoplasmonic vortices *Science* **355** 1187–91

[16] Wang H, Liu L, Zhou C, Xu J, Zhang M, Teng S and Cai Y 2019 Vortex beam generation with variable topological charge based on a spiral slit based on a spiral slit *Nanophotonics* **8** 317–24
[17] Lee S-Y, Kim S-J, Kwon H and Lee B 2015 Spin-direction control of high-order plasmonic vortex with double-ring distributed nanoslits *IEEE Photon. Technol. Lett.* **27** 705–8
[18] Wang H, Liu L, Liu C, Li X, Wang S, Xu Q and Teng S 2018 Plasmonic vortex generator without polarization dependence *New J. Phys.* **20** 033024
[19] Du L, Xie Z, Si G, Yang A, Li C, Lin J, Li G, Wang H and Yuan X 2019 On-chip photonic spin Hall lens *ACS Photon.* **6** 1840–7
[20] Chen C-F, Ku C-T, Tai Y-H, Wei P-K, Lin H-N and Huang C-B 2015 Creating optical near-field orbital angular momentum in a gold metasurface *Nano Lett.* **15** 2746–50
[21] Chen S, Cai Y, Li G, Zhang S and Cheah K W 2016 Geometric metasurface fork gratings for vortex-beam generation and manipulation *Laser Photon Rev.* **10** 322–6
[22] Tan Q, Guo Q, Liu H, Huang X and Zhang S 2017 Controlling the plasmonic orbital angular momentum by combining the geometric and dynamic phases *Nanoscale* **9** 4944–9
[23] David A, Gjonaj B and Bartal G 2016 Two-dimensional optical nanovortices at visible light *Phys. Rev.* B **93** 121302
[24] Yang Y, Wu L, Liu Y, Xie D, Jin Z, Li J, Hu G and Qiu C-W 2020 *Nano Lett.* **20** 6774–9
[25] Lu X, Han Y, Lv H, Mou Z, Zhou C, Wang S and Teng S 2020 α spiral nanoslit and the higher order plasmonic vortex generation *Nanotechnology* **31** 305201
[26] Zhou C D, Mou Z, Bao R, Li Z and Teng S Y 2021 Compound plasmonic vortex generation based on spiral nanoslits *Front. Phys.* **16** 33503
[27] Zhang Q, Wang H, Liu L and Teng S 2018 Generation of vector beams using spatial variation nanoslits with linearly polarized light illumination *Opt. Express* **26** 24145–54
[28] Teng S, Zhang Q, Wang H, Liu L and Lv H 2019 Conversion between polarization states based on a metasurface *Photon. Res.* **7** 246–50
[29] Bao R, Mou Z, Zhou C, Bai Q, He X, Han Z, Wang S and Teng S 2020 Generation of diffraction-free beams using resonant metasurfaces *New J. Phys.* **22** 103064
[30] Palik E D 1998 *Handbook of Optical Constants of Solids* (New York: Academic)